



HAL
open science

MATISSE, the VLTI mid-infrared imaging spectro-interferometer at the time of the first published astrophysical results

Stéphane Lagarde, Anthony Meilland, Bruno Lopez, Romain Petrov, Fatmé Allouche, Alexis Matter, Jean-Charles Augereau, Phillippe Berio, Felix Bettonvil, Roy van Boekel, et al.

► **To cite this version:**

Stéphane Lagarde, Anthony Meilland, Bruno Lopez, Romain Petrov, Fatmé Allouche, et al.. MATISSE, the VLTI mid-infrared imaging spectro-interferometer at the time of the first published astrophysical results. PROCEEDINGS VOLUME 12183 SPIE ASTRONOMICAL TELESCOPES + INSTRUMENTATION Optical and Infrared Interferometry and Imaging VIII 2022, Jul 2022, Montréal, Canada. pp.9, 10.1117/12.2630164 . hal-03806353

HAL Id: hal-03806353

<https://cnrs.hal.science/hal-03806353v1>

Submitted on 13 Oct 2022

HAL is a multi-disciplinary open access archive for the deposit and dissemination of scientific research documents, whether they are published or not. The documents may come from teaching and research institutions in France or abroad, or from public or private research centers.

L'archive ouverte pluridisciplinaire **HAL**, est destinée au dépôt et à la diffusion de documents scientifiques de niveau recherche, publiés ou non, émanant des établissements d'enseignement et de recherche français ou étrangers, des laboratoires publics ou privés.

MATISSE, the VLTI mid-infrared imaging spectro-interferometer at the time of the first published astrophysical results

Stéphane Lagarde^a, Anthony Meilland^a, Bruno Lopez^a, Romain G. Petrov^a, Fatmé Allouche^a, Alexis Matter^a, Jean-Charles Augereau^b, Philippe Berio^a, Felix Bettonvil^c, Roy van Boekel^d, Paul Bristow^f, Pierre Cruzalèbes^a, William C. Danchi^g, Andreas Glindemann^f, Massinissa Hadjara^h, Matthias Heiningerⁱ, Michiel Hogerheijde^j, Walter Jaffe^j, James Leftley^a, Michael Lehmitz^d, Florentin Millour^a, Claudia Paladini^e, Eric Pantin^k, Miguel Riquelme^e, Thomas Rivinius^e, Sylvie Robbe-Dubois^a, Markus Schoeller^f, Jozsef Varga^j, Gerd Weigeltⁱ, Julien Woillez^f, and Gérard Zins^f

^aLaboratoire Lagrange, Université Côte d'Azur, Observatoire de la Côte d'Azur, CNRS, CS 34229, 06304 Nice Cedex 4, France, and, MATISSE Consortium *

^bUniv. Grenoble Alpes, CNRS, IPAG, 38000 Grenoble, France

^cNOVA Optical IR Instrumentation Group at ASTRON, Netherlands

^dMax Planck Institute for Astronomy, Königstuhl 17, D-69117 Heidelberg, Germany

^eEuropean Southern Observatory, Alonso de Cordova 3107, Vitacura, Santiago, Chile

^fEuropean Southern Observatory Headquarters, Karl-Schwarzschild-Straße 2, 85748 Garching bei München, Germany

^gNASA Goddard Space Flight Center Astrophysics Science Division, Code 660, Greenbelt, MD 20771, USA

^hChinese Academy of Sciences South America Center for Astronomy, National Astronomical Observatories, CAS, Beijing 100101, China

^hMax-Planck-Institut für Radioastronomie, Auf dem Hügel 69, D-53121 Bonn, Germany

^jLeiden Observatory, Leiden University, Niels Bohrweg 2, NL-2333 CA Leiden, the Netherlands

^kAIM, CEA, CNRS, Université Paris-Saclay, Université Paris Diderot, Sorbonne Paris Cité, 91191 Gif-sur-Yvette, France

ABSTRACT

The Very Large Telescope Interferometer (VLTI) is currently the best infrastructure for long-baseline interferometry in particular in terms of sensitivity and accessibility to the general user. MATISSE, installed at the VLTI focus since end of 2017, belongs to the second generation instruments. MATISSE, the Multi AperTure mid-Infrared SpectroScopic Experiment, for the first time accesses high resolution imaging over a wide spectral domain of the mid-infrared. The instrument is a spectro-interferometric imager in the atmospheric transmission windows called L, M, and N, from 2.8 to 13.0 microns, and combines four optical beams from the VLTI's unit or auxiliary telescopes. The instrument utilises a multi-axial beam combination that delivers spectrally dispersed fringes. The signal provides the following quantities at several spectral resolutions: photometric flux, coherent flux, visibility, closure phase, wavelength differential visibility and phase, and aperture-synthesis imaging. MATISSE can operate as a stand alone instrument or with the GRA4MAT set-up employing the GRAVITY fringe tracking capabilities. The updated MATISSE performance are presented at the conference together with a selection of two front-line science topics explored since the start of the science operations in 2019. Finally we present

* MATISSE was designed, funded, and built in close collaboration with ESO by a consortium composed of institutes in France (J.-L. Lagrange Laboratory — INSU-CNRS — Côte d'Azur Observatory — the University of Nice Sophia-Antipolis), Germany (MPIA, MPIfR, and the University of Kiel), the Netherlands (NOVA and the University of Leiden), and Austria (the University of Vienna). The Konkoly Observatory and the University of Cologne have also provided support in manufacturing the instrument.

the perspective and benefit of two technical improvements foreseen in the coming years: the MATISSE-Wide off-axis fringe tracking capability and new adaptive optics for the UTs in the context of the GRAVITY+ project.

Keywords: Interferometry, mid-infrared, astrophysical results, VLTI

1. INTRODUCTION

The Multi AperTure mid-Infrared SpectroScopic Experiment, MATISSE, is the mid-infrared spectrograph and imager of the VLTI. This second generation interferometric instrument was designed with prime science objectives focusing on the Young Stellar Objects (YSOs) and on their associated stellar and planet formation processes, on the Active Galactic Nuclei (AGNs) and their active central engine, on the Stellar Physics, the surface structure and mass loss of stars at different evolutionary stages and in frequent binary interactions.

In particular, MATISSE is perfectly designed to observe the small spatial scales in YSO environments at wavelengths at which the dust material that represents the elementary bricks initiating the growth of the planet core embryos, emits efficiently. MATISSE will also be of importance to probe the inner dust structure in AGNs by testing the validity of the AGN unified model. That model is supposedly edge-on and is hiding the central source in type-II AGN and it is face-on and dominated by the inner dust sublimation radius in type-I AGN. Clumpy structures with important polar extensions are expected to trace the dust driven wind in the brightest AGNs.

MATISSE gives access to the L (2.8–4.2), M (4.5–5.0 μm) and N bands (8.0–13.0 μm) band, various spectral resolutions between R 30 and R 3500, which allow to study very specific gas and dust material spectral signatures (see Table 1). MATISSE combines four beams from the VLT's unit or auxiliary telescopes and can thus provide mid-infrared images (closure-phase aperture synthesis imaging) down to an angular resolution of about 3 mas in L band. Images are now routinely produced. Even in the case where image reconstruction are not performed through aperture synthesis and a good uv coverage approach, the access to closure phases is of considerable value since they bring new unexplored constraints in this specific wavelength domain.

Through the MATISSE project, ESO and our consortium are contributing to the new generation of mid-infrared instrumentation becoming available to the astronomical community. MATISSE is an essential piece completing a worldwide ensemble of astronomical instruments. From spectral considerations and regarding the near-infrared domain (NIR), MATISSE extends the operating wavelength range of existing instruments such as PIONIER¹ and GRAVITY,² which are both also sensitive to IR radiation but at a shorter wavelength. Moreover MATISSE complements the (sub)millimetre domain in which high angular resolution observations are covered by the radio interferometer ALMA.³ MATISSE gives access to long baseline lengths compared to the mid-infrared interferometric instrument of the Large Binocular Telescope.⁴ Note that MATISSE is thus a bridge in wavelengths as well as an exploratory path for high angular resolution in its spectral bands. That is of essential importance with the advent of the JWST⁵ and the installation of METIS, the ELT mid-infrared instrument,⁶ both of which will operate in the same wavelength domain as MATISSE. In terms of sensitivity, these instruments will have advantages over MATISSE. JWST will benefit from the absence of the atmosphere and low background observing conditions due to its location in space, while METIS will benefit from the large collecting area of the ELT. However, from an imaging point of view, MATISSE has a resolving power $20\times$ and $4\text{--}5\times$ greater than that of the JWST and METIS respectively.

2. OVERVIEW OF THE MAIN INSTRUMENT CHARACTERISTICS

MATISSE operates in three atmospheric transmission windows, the L, M, and N bands of the mid-infrared. It combines four beams coming from either the 4 UTs or the 4 ATs of the VLTI. The offered spectral bands and resolutions are presented in Tab. 1.

The MATISSE instrument (Fig. 1) consists of a warm optical system and two cold optical benches (COBs) housed in two separate cryostats, one for the L-M band, and one for the N band. The WOP operates at an ambient temperature. It is fed by four beams from the VLTI, which are propagated via dichroic beam splitters to the two COBs (Fig.2).

The MATISSE instrument contains several specific functions of importance :

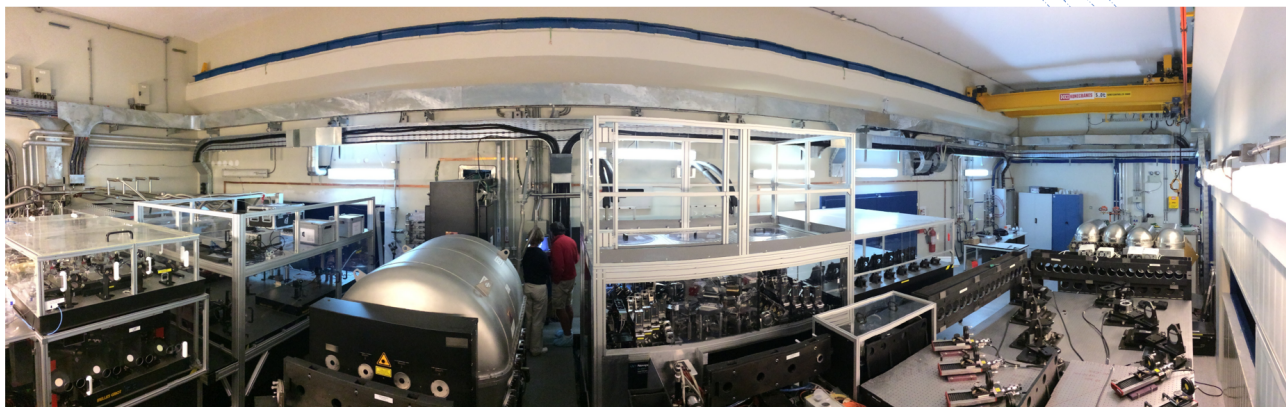
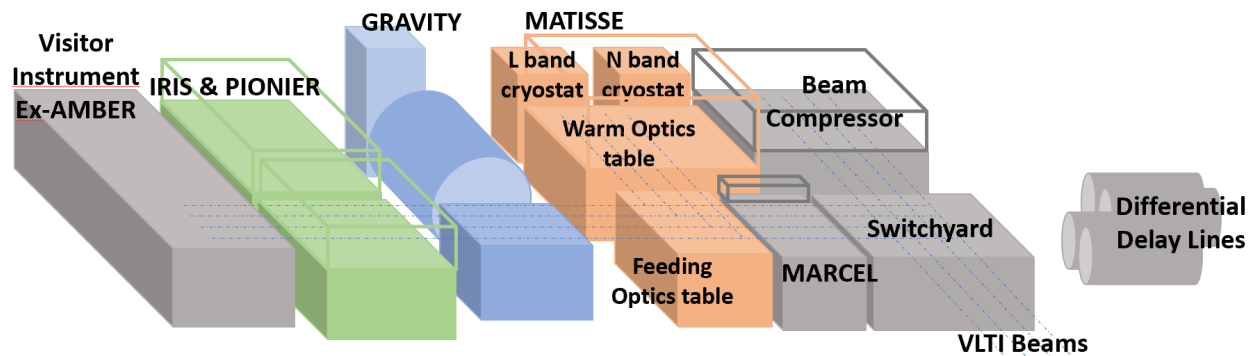


Figure 1: Top: Layout of MATISSE inside the VLT focal laboratory. In front of MATISSE, the feeding optics table reflects towards MATISSE either four UT or AT beams, after their transportation through the VLT optical train. Bottom: Location of MATISSE inside the VLT laboratory with the Warm Optics table called the WOP (and its cover) in the foreground.

Table 1: Spectral resolutions, calculated with a pinhole of $1.5\lambda/D$ in L and M band, and $2\lambda/D$ in N band.

Spectral Mode	Spectral bandwidth (μm)	Resolution
LOW-N	8.0-13.0	31.5
HIGH-N	8.0-13.0	218
LOW-LM	2.8-4.2; 4.5-5.0	31.5
MED-LM	2.8-4.2; 4.5-5.0	499
HIGH-L	2.8-4.2	979
VHIGH-L	3.95-4.2	3370
VHIGH-M	4.5-5.0	3370

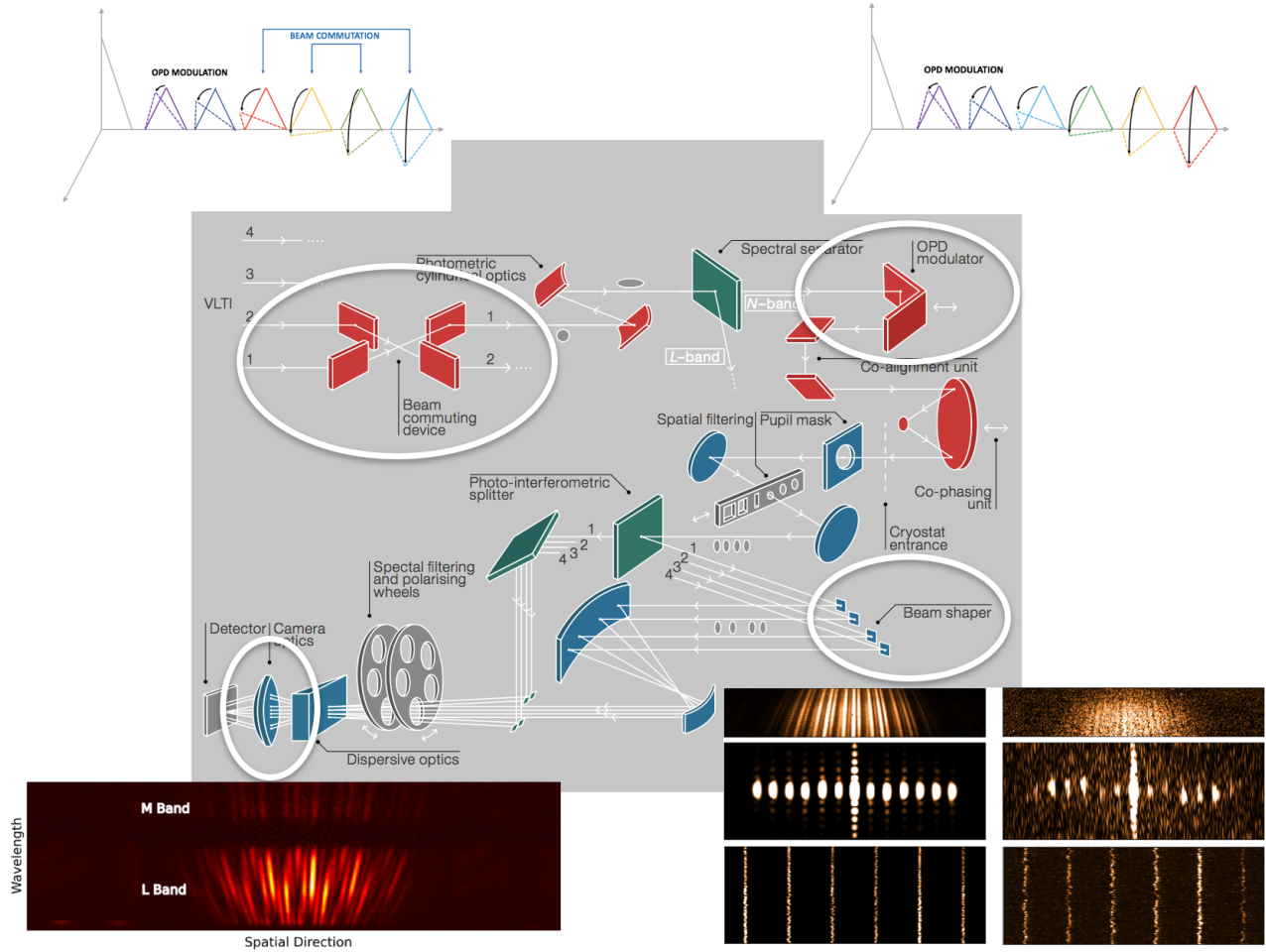


Figure 2: Sketch of the instrument with its main functions.

- the Beam Commuting Device(s): MATISSE features a specific module called Beam Commuting Device (BCD), to calibrate closure and differential phases. Two BCDs are installed at the entrance of MATISSE, one for each pair of beams. By commuting beams 1 and 2, and/or 3 and 4, we invert all the phase contributions before the instrument BCD (i.e., including the contributions of the astrophysical source, the atmosphere, and the VLTI beam trains) while keeping the instrumental contributions after the BCD device fixed. By commuting the beams, 2 differential phases and the 4 closure phases of the astrophysical object can be obtained independently of the phase produced by the instrument but not by the VLTI beam train or the atmosphere. On the closure phase, the BCDs allow a reduction of the phase residuals from several degrees to less than one degree.

- the OPD modulator(s): The thermal background contribution is huge in the mid-infrared and dominates the astrophysical signal by several orders of magnitude in N-band. In principle, it only affects the low-frequency peak of the Fourier Transform of the interferogram. However, the finite detector window and spatial variations of the detector gain can induce a crosstalk between the different peaks. Therefore, the high-frequency peaks (i.e. the fringe peaks) may be contaminated by the thermal background emission. To reduce such a contamination, a temporal modulation is performed. This modulation consists in applying an artificial Optical Path Difference (OPD) to each fringe signal with a periodic sequence during the atmospheric coherence time. It is a generalisation of the natural $0-\pi$ scheme existing with a co-axial combination. This function is provided by a set of piezo actuators. The modulation is made in ten steps of $\lambda/10$ during the coherence time in which the background remains almost constant. The resulting 10 signals are then numerically re-phased and summed. The lower frequency peak, which is not affected by the OPD modulation, and its contamination to the adjacent fringe

peaks is then eliminated and only the high frequency peaks remain.

- the beam shaper and combiner: The MATISSE beam combination is multi-axial. All the telescope beams are mixed together to produce a common interference pattern. A non-redundant beam configuration arrangement with separations between beams, respectively equal to $3D$, $9D$, and $6D$ (where D is the beam diameter), allows the fringe peaks to be separated in the Fourier space. It produces dispersed fringes on two different detectors simultaneously, the HAWAII-2RG from Teledyne Technologies for the L&M bands, and the AQUARIUS from Raytheon Company for the N band.

In the L band, the detector integration time is driven by the seeing coherence time or by the fringe tracking time (if an external fringe tracker is used). In the N band, it is driven by the high thermal background level, which imposes the individual detector integration time to be short enough to avoid saturation. Indeed the maximum exposure time in N is less than 30 ms while in L, several seconds of integration time are allowed.

The instrument has been available in open time since April 2019. Its integration at Paranal took place from November 2017 to February 2018. A two-year commissioning period followed and allowed for the instrument performance to be assessed in all modes with ATs and UTs, and within an upgraded VLTI infrastructure⁷ involving the implementation of the ATs' adaptive optics, NAOMI,⁸ and of the fringe tracker mode, GRA4MAT (Woillez et al. in preparation).

3. MAIN PERFORMANCES OF MATISSE WITH RECENT PERFORMANCE ASSESSMENTS RESULTING FROM 2022 COMMISSIONING SESSION

MATISSE is a highly sensitive spectro-interferometer⁹ which benefits from the large telescope apertures of the VLT. The ATs and the UTs are large-sized telescopes when compared to other worldwide interferometric array. This is important for mid-infrared observations which requires strong source signal at the detector level to beat the photons and background fluctuation noise generated in this spectral domain by both the atmosphere and the optical train emission.

The different contributions to the errors, which affect the measurements, are:

- The fundamental noise errors that affect the precision of all measurements.
- The broad-band seeing errors that affect the absolute visibility and closure phase independently from the source brightness.
- The broad-band photometric errors likely caused by imperfect thermal background subtraction, which produce a source flux dependent error in the absolute visibilities.
- The group delay estimation error that introduces a bias on the coherent flux, in the case of coherent integration, for faint targets.
- The chromatic OPD that has a strong impact on the differential phase

Tables 2 and 3 combine all these error sources and shows our updated estimates without fringe tracking recently reassessed considering the recent and final results of the commissioning. This limiting magnitudes correspond to the ones offered by ESO to the community of users. They are set by the following precision criteria, to be achieved per spectral channel after one minute of observation:

- Visibility: $\sigma_V = 0.1$
- Closure phase: $\sigma_\psi = 5^\circ$
- Differential phase: $\sigma_\varphi = 4^\circ$

Table 2: MATISSE standalone (i.e. without Fringe Tracker) sensitivity limits in Jy in L and M, as defined for the following precision criteria: $\sigma_V = 0.1$, $\sigma_\psi = 5^\circ$ and $\sigma_\varphi = 4^\circ$, to be achieved per spectral channel after one minute of observation. The symbol ”-” means that the combination resolution-versus-band does not exist. Magnitude 0 in L (at $3.5\mu m$) and M (at $4.75\mu m$) corresponds to $290Jy$ and $165Jy$ respectively.

Telescopes	Resolution	V		ψ		φ	
		L	M	L	M	L	M
ATs	LOW	1.1	2.1	0.4	1.9	0.3	1.1
	MED	3.8	13.2	3.3	11.5	2.4	8.4
	HIGH	20.1	-	14.7	-	10.7	-
UTs	LOW	0.3	0.4	0.07	0.15	0.06	0.15
	MED	1.1	1.1	0.8	0.9	0.6	0.7
	HIGH	2.4	-	1.7	-	1.2	-

Table 3: MATISSE standalone (i.e. without Fringe Tracker) sensitivity limits in Jy in N1 ($8.5\mu m$), N2($10.5\mu m$), N3($11.5\mu m$) as defined for the following precision criteria: $\sigma_V = 0.1$, $\sigma_\psi = 5^\circ$ and $\sigma_\varphi = 4^\circ$, to be achieved per spectral channel after one minute of observation. Magnitude 0 in N (at $8.5\mu m$) corresponds to $50Jy$.

Telescopes	Resolution	V			ψ			φ		
		N1	N2	N3	N1	N2	N3	N1	N2	N3
ATs	LOW	16.8	31.4	44.0	9.4	23.6	36.7	2.9	7.5	11.7
	HIGH	30.3	51.3	83.7	29.9	-	-	25.3	45.9	58.9
UTs	LOW	0.9	1.4	1.9	0.3	0.8	1.3	0.2	0.55	0.6
	HIGH	1.6	3.4	4.1	1.5	-	-	1.1	3.5	3.7

4. A SELECTION OF RECENTLY PUBLISHED RESULTS

MATISSE was designed as a successor to MIDI, a prolific instrument which produced numerous results on protoplanetary disks, AGNs, and evolved stars. Beyond its huge success, MIDI was nevertheless limited to two telescopes. Going from a two-beam to a four-beam combiner increases the number of simultaneous visibility measurements by a factor 6 and gives access to closure phase measurements. Moreover, MATISSE also opens two new spectral windows at VLTI, the L and M bands, filling the gap of the first generation VLTI instruments. Its very extended spectral domain allows to probe dust, from the sublimation temperature down to about 200K, and free-free emission from hot gas. Moreover, by using its various spectral resolutions, solid-state features, molecular bands and atomic lines can be spectrally resolved, allowing to spatially disentangle gas and dust emissions, constrain their physics, infer the dust mineralogy and even probe the gas kinematics.

In Fig. 3 we present three of the first reconstructed images from MATISSE: the circumstellar disk around the unclassified B[e] star FS CMa,¹⁰ the dusty torus around the AGN NGC 1068,¹¹ and the spectro-imaging in the Br α emission line of the wind collision zone around the massive binary star η Car.¹² These images not only demonstrate the capability of MATISSE to image environment at a few milli-arcseconds resolution, but also its ability to produce spectrally-resolved images either in a large spectral domain (from 3 to 13 μm) in the case of FS CMa and NGC 1068 or at a resolution high enough to study kinematics in spectral lines in the case of η Car ($R \gtrsim 1000$).

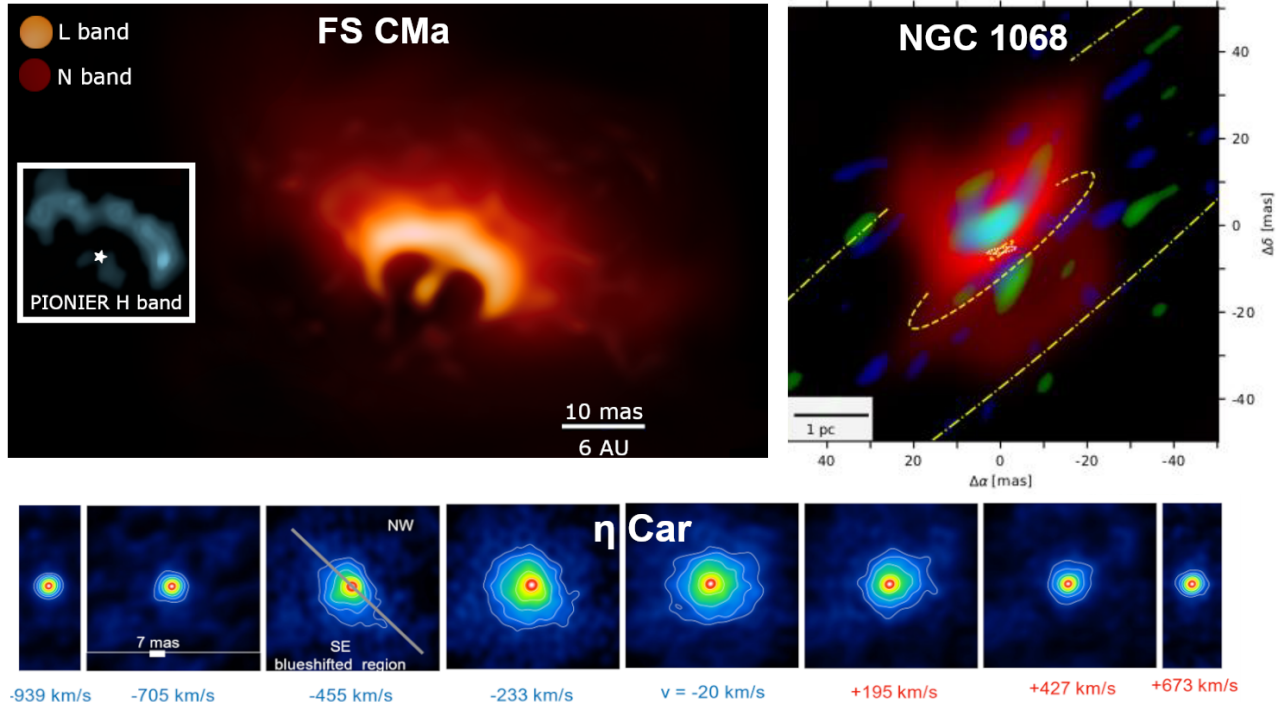


Figure 3: A few of the first Images reconstructed from MATISSE observations. Top left: the circumstellar Disk around the unclassified B[e] star FS CMa.¹⁰ Top Right: NGC1068 dusty torus.¹¹ Bottom : spectro-imaging in the Br α emission line of the wind collision zone around the massive binary star η Car.¹²

Thanks to its high spatial resolution MATISSE can access the decisive mas scale, which translates to the pc at the typical distance of the closest AGNs (\sim Mpc). As shown by the image of NGC1068 presented in Fig 3 but also by the one on Circinus published in ¹³, MATISSE can image the inner dust structure in AGNs and challenge the simple 'dust torus' model of the AGN unified model. That model is supposedly edge-on and hiding the central source in type-II AGNs while it is face-on and dominated by the inner dust sublimation radius in type-I AGNs. Clumpy structures with important polar extensions are expected to trace the dusty wind driven by radiation pressure in the brightest AGNs¹⁴. The 2-telescope MIDI instrument was unable to make images and could only give angular sizes as a function of the position angle. It was limited to the N band where it is difficult to discriminate the effects of the temperature and composition of the emitting dust from the foreground absorbing medium. MATISSE solves these two problems by making images in the N band where dust emission dominates. The inner dust structure in AGN is the tracer of the exchanges between the central engine, its surrounding broad line region (BLR), and the host galaxy. Observing it down to the pc scale can reveal the mechanisms of co-evolution of the super massive black holes and galaxies. Moreover, understanding the geometry of the nuclei well can allow independent distance estimates in combination with infrared (IR) reverberation mapping¹⁵. Finally, the recent breakthrough made by GRAVITY on the spectro-astrometry of BLRs¹⁶ makes this MATISSE information of an even higher value.

In the case of YSOs and protoplanetary disks, reaching the mas scale in the mid-infrared allows to probe au or even sub-au scale for the closest star-forming regions (\sim 150 pc). Notably, accessing that spatial scale is required to resolve the water ice line in disks, which is thought to represent the outer boundary of the telluric planet forming region. In addition, mapping disks at such a spatial scale could allow to detect au-scale gaps or radial-inhomogeneities that could be linked to planet formation. A survey is being conducted by the MATISSE consortium and more than 60 young stars have been observed as of July 2022. one example of star observed in the frame of this survey is the Herbig Ae star HD 163296¹⁷. MATISSE obser-

vations revealed a significant brightness asymmetry in the L-band emission at a very small scale, i.e., 0.33 ± 0.01 au. The authors proposed that this asymmetric structure, located in or near the inner rim of the dusty disk, orbits the star. To find the physical origin of the asymmetry, they tested the hypothesis of a vortex created by a Rossby wave instability. They found that a unique large-scale vortex is compatible with the MATISSE data. Such vortices are typically proposed as a mechanism to trap dust particles and facilitate planetesimal growth in proto-planetary discs.

Another important matter regarding YSOs is to trace carbon in their protoplanetary disks. While detected in the outer disk regions, little is known about the solid carbon species in the inner disk regions and key questions are whether there is a significant reservoir of C-based solid species in the inner 10 au region of disks, in what form are those C-based species and how can solid carbon be incorporated into planetesimals and ultimately planets. Thanks to its large wavelength coverage (3-13 μ m) and using its medium spectral resolution mode (R>500) MATISSE can study various carbonaceous molecules and nanograins (PAHs, nano-diamonds, CO) down to the sub-au scale.

In¹⁸, MATISSE observations allowed to detect the presence of two separated carbonaceous dust populations in the disk around the Herbig star HD 179218: very hot nano-grains that dominate the near-to mid-IR emission in the inner optically thin 10 au region and colder and larger grains that dominate the emission outward. The survival of nano-grains in the highly irradiated inner 10 au region brings new insights in the different photo-induced processes acting on such small grains, and their regeneration/replenishment: accretion could maintain a significant inflow of material to maintain a stable nano-grain population there as well as local photo-fragmentation of larger carbonaceous grains.

In parallel to the two main drivers that are YSOs and AGNs, MATISSE has started to produce many results in the field of evolved stars. MATISSE can image dusty and gaseous circumstellar environments around hot stars such as the ones presented in 3 but it can also probe the surface of giant and supergiants stars as shown in¹⁹ in the case of the enigmatic evolved star VX Sgr. In that case MATISSE observations allowed to reconstruct multi-band images of the stellar surface and compare them to outputs from radiative transfer models of both RSG and AGB star, showing that this object belong most likely to the later class of objects.

Another example is the case of the AGB star R Scl. By modeling its extended atmosphere,²⁰ managed to disentangle the emission from different chemical species (acetylene, Hydrogen cyanide, and amorphous carbon and silicon carbide dust). They showed that the molecules are located closer to the star than the dust, as shown in Fig 4, which presents the spectro-radial profiles of R Scl derived from the MATISSE data. Such pioneering work will help to improve our understanding of the chemical process around AGBs star and dust formation.

5. FORESEEN VLTI UPGRADES FOR FRONTLINE SCIENCE

The MATISSE instrument is now routinely operating at Paranal for science observations and will soon become officially property of ESO. Indeed, the PAC (Provisional Acceptance in Chile) phase, which represents the final delivery step of the Consortium, is being concluded. Beyond the PAC, the already engaged commissioning activity on GRA4MAT will be pursued during 2022 and future upgrades are foreseen. They concern the MATISSE-Wide mode, which is the use of GRAVITY as a wide field-of-view off-axis fringe tracker for MATISSE, and the proposition of a new generation fringe tracking of the HFT-type (Petrov et al. 2022, this conference). The MATISSE-wide upgrade consists in using the so-called beam B for MATISSE and IRIS while the set of beam A are used to feed GRA4MAT (see Figure 5). The proposition of a new generation fringe tracking of the HFT-type consists in developing a dedicated fringe tracker for MATISSE and the VLTI. This was foreseen years ago by ESO at the beginning of the MATISSE Phase A. Such a new development would be to take advantage of the state-of-Art knowledge in this field by using in particular several spectral bands in once to fringe sense with the highest performance the signal (Petrov et al. 2022, this conference).

These upgrades are science driven by a major case which is the access to a much larger number of AGNs and Quasars²¹ through a multispectral approach at the VLTI. The mid-infrared domain covered by MATISSE offers crucial constraints to determine temperature maps and morphologies, and will contribute in particular by this mean to better constraints on the distance estimates through reverberation mapping methods. It is the

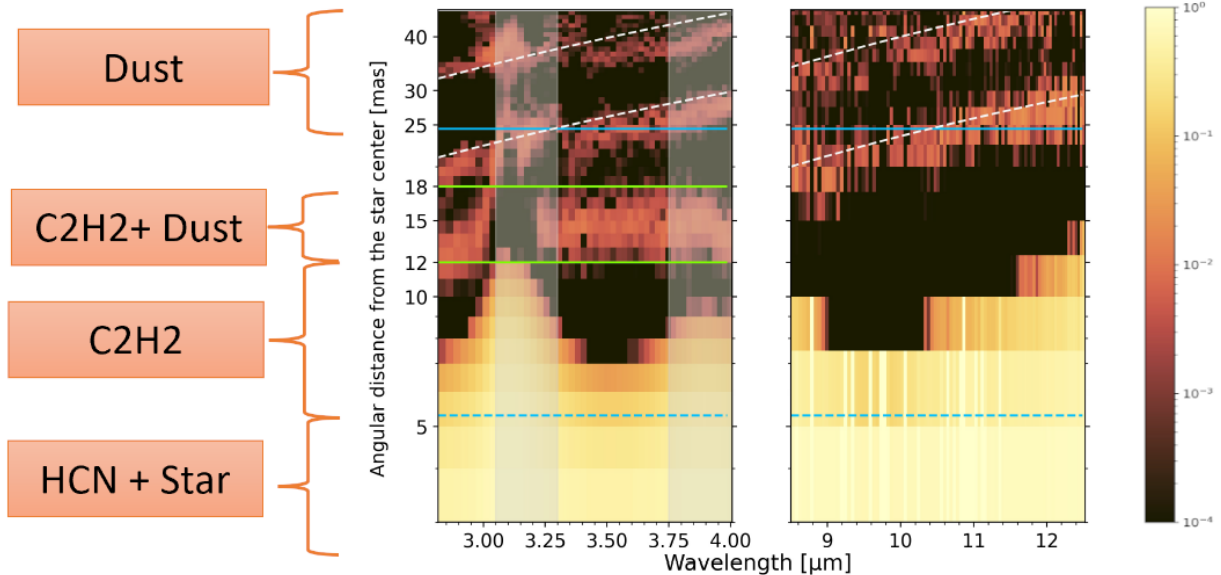


Figure 4: R Scl spectro-radial maps in L-and-N-bands²⁰ obtained by plotting the best intensity Hankel profile normalized at one for each observed wavelength. The modelling reveals the location of different species detected in the upper atmosphere and various shells around the star: hydrogen cyanide (HCN), acetylene (C_2H_2), and dust

combination of off-axis tracking through MATISSE-Wide and fringe sensing sensitivity that will deeply enlarge the studied AGN sample as demonstrated by Petrov (2022).

Through the MATISSE-wide upgrade, it is not only MATISSE performance which will be improved for faint object observations but it is globally the VLTI multi-spectral capability which will be increased to an homogeneous level allowing the community to continue to use the ensemble of instruments PIONIER, GRAVITY and MATISSE for the multi-spectral analysis of the individual sources.

REFERENCES

- [1] Zins, G., Lazareff, B., Berger, J. P., Le Bouquin, J. B., Jocou, L., Rochat, S., Haguenaer, P., Knudstrup, J., Lizon, J. L., Millan-Gabet, R., Traub, W., Benisty, M., Delboulbe, A., Feautrier, P., Gillier, D., Gitton, P., Kern, P., Kiekebusch, M., Labeye, P., Maurel, D., Magnard, Y., Micallef, M., Michaud, L., Moulin, T., Popovic, D., Roux, A., and Ventura, N., “PIONIER: A Four-telescope Instrument for the VLTI,” *The Messenger* **146**, 12–17 (Dec. 2011).
- [2] Gravity Collaboration, “First Light for GRAVITY: A New Era for Optical Interferometry,” *The Messenger* **170**, 10–15 (Dec. 2017).
- [3] Carpenter, J., Iono, D., Kemper, F., and Wootten, A., “The ALMA Development Program: Roadmap to 2030,” *arXiv e-prints*, arXiv:2001.11076 (Jan. 2020).
- [4] Sallum, S., Eisner, J. A., Stone, J. M., Dietrich, J., Hinz, P., and Spalding, E., “ELT Imaging of MWC 297 from the 23 m LBTI: Complex Disk Structure and a Companion Candidate,” *AJ* **161**, 28 (Jan. 2021).
- [5] Rieke, G., Wright, G. S., and MIRI Science Team, “Building the Mid-Infrared Instrument for JWST,” in [*American Astronomical Society Meeting Abstracts*], *American Astronomical Society Meeting Abstracts* **209**, 210.06 (Dec. 2006).
- [6] Brandl, B. R., Quanz, S., Snellen, I., van Dishoeck, E., Pontoppidan, K., Le Floch, E., Bettonvil, F., van Boekel, R., Glauser, A., and Hurtado, N., “The Mid-IR ELT Imager and Spectrograph (METIS) and its Science Goals in the Context of AKARI,” in [*The Cosmic Wheel and the Legacy of the AKARI Archive: From Galaxies and Stars to Planets and Life*], Ootsubo, T., Yamamura, I., Murata, K., and Onaka, T., eds., 41–47 (Mar. 2018).

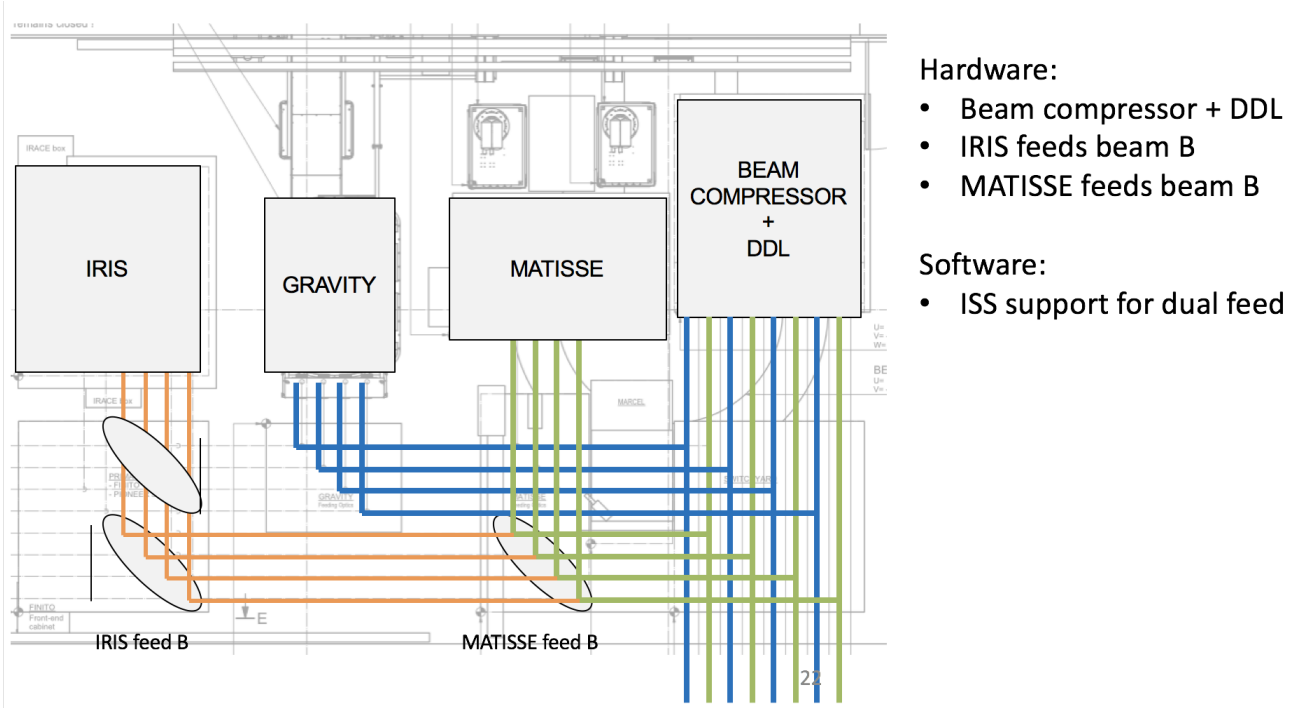


Figure 5: Sketch of the MATISSE feeding optics setup allowing the off-axis use of GRA4MAT.

- [7] Woillez, J., Gonté, F., Abad, J. A., Abadie, S., Abuter, R., Accardo, M., Acuña, M., Alonso, J., Andolfato, L., Avila, G., Barriga, P. J., Beltran, J., Berger, J. P., Bollados, C., Bourget, P., Brast, R., Bristow, P., Caniguante, L., Castillo, R., Conzelmann, R., Cortes, A., Delplancke, F., Dell Valle, D., Derie, F., Diaz, A., Donoso, R., Duhoux, P., Dupuy, C., Elao, C., Egner, S., Fuentesecca, E., Fernandez, R., Gaytan, D., Glindemann, A., Gonzales, J., Guisard, S., Hagenauer, P., Haimerl, A., Heinz, V., Henriquez, J. P., van der Heyden, P., Hubin, N., Huerta, R., Jochum, L., Kirchbauer, J. P., Leiva, A., Lévêque, S., Lizon, J. P., Luco, F., Mardones, P., Mellado, A., Mérand, A., Osorio, J., Ott, J., Pallanca, L., Pavez, M., Pasquini, L., Percheron, I., Pirard, J. F., Phan, D. T., Pineda, J. C., Pino, A., Poupar, S., Ramírez, A., Reïnero, C., Riquelme, M., Romero, J., Rivinius, T., Rojas, C., Rozas, F., Salgado, F., Schöller, M., Schuhler, N., Siclari, W., Stephan, C., Tamblay, R., Tapia, M., Tristram, K., Valdes, G., de Wit, W. J., Wright, A., and Zins, G., “VLTI: First Light for the Second Generation,” *The Messenger* **162**, 16–18 (Dec. 2015).
- [8] Woillez, J., Abad, J. A., Abuter, R., Aller Carpentier, E., Alonso, J., Andolfato, L., Barriga, P., Berger, J. P., Beuzit, J. L., Bonnet, H., Bourdarot, G., Bourget, P., Brast, R., Caniguante, L., Cottalorda, E., Darré, P., Delabre, B., Delboulbé, A., Delplancke-Ströbele, F., Dembet, R., Donaldson, R., Dorn, R., Dupeyron, J., Dupuy, C., Egner, S., Eisenhauer, F., Fischer, G., Frank, C., Fuentesecca, E., Gitton, P., Gonté, F., Guerlet, T., Guieu, S., Gutierrez, P., Haguenaue, P., Haimerl, A., Haubois, X., Heritier, C., Huber, S., Hubin, N., Jolley, P., Jocu, L., Kirchbauer, J. P., Kolb, J., Kosmalski, J., Krempf, P., Le Bouquin, J. B., Le Louarn, M., Lilley, P., Lopez, B., Magnard, Y., Mclay, S., Meilland, A., Meister, A., Merand, A., Moulin, T., Pasquini, L., Paufique, J., Percheron, I., Pettazzi, L., Pfuhl, O., Phan, D., Pirani, W., Quentin, J., Rakich, A., Ridings, R., Riedel, M., Reyes, J., Rochat, S., Santos Tomás, G., Schmid, C., Schuhler, N., Shcheketurov, P., Seidel, M., Soenke, C., Stadler, E., Stephan, C., Suárez, M., Todorovic, M., Valdes, G., Verinaud, C., Zins, G., and Zúñiga-Fernández, S., “NAOMI: the adaptive optics system of the Auxiliary Telescopes of the VLTI,” *A&A* **629**, A41 (Sept. 2019).
- [9] Lopez, B., Lagarde, S., Petrov, R. G., Jaffe, W., Antonelli, P., Allouche, F., Berio, P., Matter, A., Meilland, A., Millour, F., Robbe-Dubois, S., Henning, T., Weigelt, G., Glindemann, A., Agocs, T., Bailet, C., Beckmann, U., Bettonvil, F., van Boekel, R., Bourget, P., Bresson, Y., Bristow, P., Cruzalèbes, P., Eldswijk, E., Fantéi Caujolle, Y., González Herrera, J. C., Graser, U., Guajardo, P., Heininger, M., Hofmann, K. H.,

Kroes, G., Laun, W., Lehmitz, M., Leinert, C., Meisenheimer, K., Morel, S., Neumann, U., Paladini, C., Percheron, I., Riquelme, M., Schoeller, M., Stee, P., Venema, L., Woillez, J., Zins, G., Ábrahám, P., Abadie, S., Abuter, R., Accardo, M., Adler, T., Alonso, J., Augereau, J. C., Böhm, A., Bazin, G., Beltran, J., Bensberg, A., Boland, W., Brast, R., Burtscher, L., Castillo, R., Chelli, A., Cid, C., Clausse, J. M., Connot, C., Conzelmann, R. D., Danchi, W. C., Delbo, M., Drevon, J., Dominik, C., van Duin, A., Ebert, M., Eisenhauer, F., Flament, S., Frahm, R., Gámez Rosas, V., Gabasch, A., Gallenne, A., Garces, E., Girard, P., Glazenberg, A., Gonté, F. Y. J., Guitton, F., de Haan, M., Hanenburg, H., Haubois, X., Hocdé, V., Hogerheijde, M., ter Horst, R., Hron, J., Hummel, C. A., Hubin, N., Huerta, R., Idserda, J., Isbell, J. W., Ives, D., Jakob, G., Jaskó, A., Jochum, L., Klarmann, L., Klein, R., Kragt, J., Kuindersma, S., Kokoulina, E., Labadie, L., Lacour, S., Leftley, J., Le Poole, R., Lizon, J. L., Lopez, M., Lykou, F., Mérand, A., Marcotto, A., Mauclet, N., Maurer, T., Mehrgan, L. H., Meisner, J., Meixner, K., Mellein, M., Menut, J. L., Mohr, L., Mosoni, L., Navarro, R., Nußbaum, E., Pallanca, L., Pantin, E., Pasquini, L., Phan Duc, T., Pott, J. U., Pozna, E., Richichi, A., Ridinger, A., Rigal, F., Rivinius, T., Roelfsema, R., Rohloff, R. R., Rousseau, S., Salabert, D., Schertl, D., Schuhler, N., Schuil, M., Shabun, K., Soulain, A., Stephan, C., Toledo, P., Tristram, K., Tromp, N., Vakili, F., Varga, J., Vinther, J., Waters, L. B. F. M., Wittkowski, M., Wolf, S., Wrhel, F., and Yoffe, G., “MATISSE, the VLTI mid-infrared imaging spectro-interferometer,” *Astronomy & Astrophysics* **659**, A192 (Mar. 2022).

- [10] Hofmann, K. H., Bensberg, A., Schertl, D., Weigelt, G., Wolf, S., Meilland, A., Millour, F., Waters, L. B. F. M., Kraus, S., Ohnaka, K., Lopez, B., Petrov, R. G., Lagarde, S., Berio, P., Allouche, F., Robbe-Dubois, S., Jaffe, W., Henning, T., Paladini, C., Schöller, M., Mérand, A., Glindemann, A., Beckmann, U., Heininger, M., Bettonvil, F., Zins, G., Woillez, J., Bristow, P., Stee, P., Vakili, F., van Boekel, R., Hogerheijde, M. R., Dominik, C., Augereau, J. C., Matter, A., Hron, J., Pantin, E., Rivinius, T., de Wit, W. J., Varga, J., Klarmann, L., Meisenheimer, K., Gámez Rosas, V., Burtscher, L., Leftley, J., Isbell, J. W., Yoffe, G., Kokoulina, E., Danchi, W. C., Cruzalèbes, P., Domiciano de Souza, A., Drevon, J., Hocdé, V., Kreplin, A., Labadie, L., Connot, C., Nußbaum, E., Lehmitz, M., Antonelli, P., Graser, U., and Leinert, C., “VLTI-MATISSE L- and N-band aperture-synthesis imaging of the unclassified B[e] star FS Canis Majoris,” *Astronomy & Astrophysics* **658**, A81 (Feb. 2022).
- [11] Gámez Rosas, V., Isbell, J. W., Jaffe, W., Petrov, R. G., Leftley, J. H., Hofmann, K.-H., Millour, F., Burtscher, L., Meisenheimer, K., Meilland, A., Waters, L. B. F. M., Lopez, B., Lagarde, S., Weigelt, G., Berio, P., Allouche, F., Robbe-Dubois, S., Cruzalèbes, P., Bettonvil, F., Henning, T., Augereau, J.-C., Antonelli, P., Beckmann, U., van Boekel, R., Bendjoya, P., Danchi, W. C., Dominik, C., Drevon, J., Gallimore, J. F., Graser, U., Heininger, M., Hocdé, V., Hogerheijde, M., Hron, J., Impellizzeri, C. M. V., Klarmann, L., Kokoulina, E., Labadie, L., Lehmitz, M., Matter, A., Paladini, C., Pantin, E., Pott, J.-U., Schertl, D., Soulain, A., Stee, P., Tristram, K., Varga, J., Woillez, J., Wolf, S., Yoffe, G., and Zins, G., “Thermal imaging of dust hiding the black hole in NGC 1068,” *Nature* **602**, 403–407 (Feb. 2022).
- [12] Weigelt, G., Hofmann, K. H., Schertl, D., Lopez, B., Petrov, R. G., Lagarde, S., Berio, P., Jaffe, W., Henning, T., Millour, F., Meilland, A., Allouche, F., Robbe-Dubois, S., Matter, A., Cruzalèbes, P., Hillier, D. J., Russell, C. M. P., Madura, T., Gull, T. R., Corcoran, M. F., Damineli, A., Moffat, A. F. J., Morris, P. W., Richardson, N. D., Paladini, C., Schöller, M., Mérand, A., Glindemann, A., Beckmann, U., Heininger, M., Bettonvil, F., Zins, G., Woillez, J., Bristow, P., Sanchez-Bermudez, J., Ohnaka, K., Kraus, S., Mehner, A., Wittkowski, M., Hummel, C. A., Stee, P., Vakili, F., Hartman, H., Navarete, F., Hamaguchi, K., Espinoza-Galeas, D. A., Stevens, I. R., van Boekel, R., Wolf, S., Hogerheijde, M. R., Dominik, C., Augereau, J. C., Pantin, E., Waters, L. B. F. M., Meisenheimer, K., Varga, J., Klarmann, L., Gámez Rosas, V., Burtscher, L., Leftley, J., Isbell, J. W., Hocdé, V., Yoffe, G., Kokoulina, E., Hron, J., Groh, J., Kreplin, A., Rivinius, T., de Wit, W. J., Danchi, W. C., Domiciano de Souza, A., Drevon, J., Labadie, L., Connot, C., Nußbaum, E., Lehmitz, M., Antonelli, P., Graser, U., and Leinert, C., “VLTI-MATISSE chromatic aperture-synthesis imaging of η Carinae’s stellar wind across the Br α line. Periastron passage observations in February 2020,” *Astronomy & Astrophysics* **652**, A140 (Aug. 2021).
- [13] Isbell, J. W., Meisenheimer, K., Pott, J. U., Stalevski, M., Tristram, K. R. W., Sanchez-Bermudez, J., Hofmann, K. H., Gámez Rosas, V., Jaffe, W., Burtscher, L., Leftley, J., Petrov, R., Lopez, B., Henning, T., Weigelt, G., Allouche, F., Berio, P., Bettonvil, F., Cruzalèbes, P., Dominik, C., Heininger, M., Hogerheijde, M., Lagarde, S., Lehmitz, M., Matter, A., Meilland, A., Millour, F., Robbe-Dubois, S., Schertl, D., van

- Boekel, R., Varga, J., and Woillez, J., “The dusty heart of Circinus. I. Imaging the circumnuclear dust in N-band,” *Astronomy & Astrophysics* **663**, A35 (July 2022).
- [14] Leftley, J. H., Tristram, K. R. W., Hönic, S. F., Kishimoto, M., Asmus, D., and Gandhi, P., “New Evidence for the Dusty Wind Model: Polar Dust and a Hot Core in the Type-1 Seyfert ESO 323-G77,” *The Astrophysical Journal* **862**, 17 (July 2018).
- [15] Hönic, S. F., Watson, D., Kishimoto, M., and Hjorth, J., “A dust-parallax distance of 19 megaparsecs to the supermassive black hole in NGC 4151,” *Nature* **515**, 528–530 (Nov. 2014).
- [16] Gravity Collaboration, Sturm, E., Dexter, J., Pfuhl, O., Stock, M. R., Davies, R. I., Lutz, D., Clénet, Y., Eckart, A., Eisenhauer, F., Genzel, R., Gratadour, D., Hönic, S. F., Kishimoto, M., Lacour, S., Millour, F., Netzer, H., Perrin, G., Peterson, B. M., Petrucci, P. O., Rouan, D., Waisberg, I., Woillez, J., Amorim, A., Brandner, W., Förster Schreiber, N. M., Garcia, P. J. V., Gillessen, S., Ott, T., Paumard, T., Perraut, K., Scheithauer, S., Straubmeier, C., Tacconi, L. J., and Widmann, F., “Spatially resolved rotation of the broad-line region of a quasar at sub-parsec scale,” *Nature* **563**, 657–660 (Nov. 2018).
- [17] Varga, J., Hogerheijde, M., van Boekel, R., Klarmann, L., Petrov, R., Waters, L. B. F. M., Lagarde, S., Pantin, E., Berio, P., Weigelt, G., Robbe-Dubois, S., Lopez, B., Millour, F., Augereau, J. C., Meheut, H., Meilland, A., Henning, T., Jaffe, W., Bettonvil, F., Bristow, P., Hofmann, K. H., Matter, A., Zins, G., Wolf, S., Allouche, F., Donnan, F., Schertl, D., Dominik, C., Heininger, M., Lehmitz, M., Cruzalèbes, P., Glindemann, A., Meisenheimer, K., Paladini, C., Schöller, M., Woillez, J., Venema, L., Kokoulina, E., Yoffe, G., Ábrahám, P., Abadie, S., Abuter, R., Accardo, M., Adler, T., Agócs, T., Antonelli, P., Böhm, A., Bailet, C., Bazin, G., Beckmann, U., Beltran, J., Boland, W., Bourget, P., Brast, R., Bresson, Y., Burtscher, L., Castillo, R., Chelli, A., Cid, C., Clausse, J. M., Connot, C., Conzelmann, R. D., Danchi, W. C., De Haan, M., Delbo, M., Ebert, M., Elswijk, E., Fantei, Y., Frahm, R., Gámez Rosas, V., Gabasch, A., Gallenne, A., Garces, E., Girard, P., Gonté, F. Y. J., González Herrera, J. C., Graser, U., Guajardo, P., Guitton, F., Haubois, X., Hron, J., Hubin, N., Huerta, R., Isbell, J. W., Ives, D., Jakob, G., Jaskó, A., Jochum, L., Klein, R., Kragt, J., Kroes, G., Kuindersma, S., Labadie, L., Laun, W., Le Poole, R., Leinert, C., Lizon, J. L., Lopez, M., Mérand, A., Marcotto, A., Mauclet, N., Maurer, T., Mehrgan, L. H., Meisner, J., Meixner, K., Mellein, M., Mohr, L., Morel, S., Mosoni, L., Navarro, R., Neumann, U., Nußbaum, E., Pallanca, L., Pasquini, L., Percheron, I., Pott, J. U., Pozna, E., Ridinger, A., Rigal, F., Riquelme, M., Rivinius, T., Roelfsema, R., Rohloff, R. R., Rousseau, S., Schuhler, N., Schuil, M., Soulain, A., Stee, P., Stephan, C., ter Horst, R., Tromp, N., Vakili, F., van Duin, A., Vinther, J., Wittkowski, M., and Wrhel, F., “The asymmetric inner disk of the Herbig Ae star HD 163296 in the eyes of VLTI/MATISSE: evidence for a vortex?,” *Astronomy & Astrophysics* **647**, A56 (Mar. 2021).
- [18] Kokoulina, E., Matter, A., Lopez, B., Pantin, E., Ysard, N., Weigelt, G., Habart, E., Varga, J., Jones, A., Meilland, A., Dartois, E., Klarmann, L., Augereau, J. C., van Boekel, R., Hogerheijde, M., Yoffe, G., Waters, L. B. F. M., Dominik, C., Jaffe, W., Millour, F., Henning, T., Hofmann, K. H., Schertl, D., Lagarde, S., Petrov, R. G., Antonelli, P., Allouche, F., Berio, P., Robbe-Dubois, S., Ábrahám, P., Beckmann, U., Bensberg, A., Bettonvil, F., Bristow, P., Cruzalèbes, P., Danchi, W. C., Dannhoff, M., Graser, U., Heininger, M., Labadie, L., Lehmitz, M., Leinert, C., Meisenheimer, K., Paladini, C., Percheron, I., Stee, P., Woillez, J., Wolf, S., Zins, G., Delbo, M., Drevon, J., Duprat, J., Gámez Rosas, V., Hocdé, V., Hron, J., Hummel, C. A., Isbell, J. W., Leftley, J., Soulain, A., Vakili, F., and Wittkowski, M., “First MATISSE L-band observations of HD 179218. Is the inner 10 au region rich in carbon dust particles?,” *Astronomy & Astrophysics* **652**, A61 (Aug. 2021).
- [19] Chiavassa, A., Kravchenko, K., Montargès, M., Millour, F., Matter, A., Freytag, B., Wittkowski, M., Hocdé, V., Cruzalèbes, P., Allouche, F., Lopez, B., Lagarde, S., Petrov, R. G., Meilland, A., Robbe-Dubois, S., Hofmann, K. H., Weigelt, G., Berio, P., Bendjoya, P., Bettonvil, F., Domiciano de Souza, A., Heininger, M., Henning, T., Isbell, J. W., Jaffe, W., Labadie, L., Lehmitz, M., Meisenheimer, K., Soulain, A., Varga, J., Augereau, J. C., van Boekel, R., Burtscher, L., Danchi, W. C., Dominik, C., Drevon, J., Gámez Rosas, V., Hogerheijde, M. R., Hron, J., Klarmann, L., Kokoulina, E., Lagadec, E., Leftley, J., Mosoni, L., Nardetto, N., Paladini, C., Pantin, E., Schertl, D., Stee, P., Szabados, L., Waters, R., Wolf, S., and Yoffe, G., “The extended atmosphere and circumstellar environment of the cool evolved star VX Sagittarii as seen by MATISSE,” *Astronomy & Astrophysics* **658**, A185 (Feb. 2022).

- [20] Drevon, J., “Locating dust and molecules in the inner circumstellar environment of R Sculptoris with MATISSE,” *Astronomy & Astrophysics* -, - (2022).
- [21] Boskri, A., Petrov, R. G., El Halkouj, T., Hadjara, M., Leftley, J., Benkhaldoun, Z., Cruzalèbes, P., Ziad, A., and Carillet, M., “Potential and sky coverage for off-axis fringe tracking in optical long baseline interferometry,” **506**, 1364–1388 (Sept. 2021).